

On the hadronic origin of the TeV radiation from GRB 190114C

Silvia Gagliardini^{1,2,3} Silvia Celli^{1,2}, Dafne Guetta³ Angela Zegarelli^{1,2,4} Antonio Capone^{2,3} Irene Di Palma^{1,2}

¹Dipartimento di Fisica dell'Università La Sapienza, P. le Aldo Moro 2, I-00185 Rome, Italy

²Istituto Nazionale di Fisica Nucleare, Sezione di Roma, P. le Aldo Moro 2, I-00185 Rome, Italy

³Department of Physics, Ariel University, Ariel, Israel

⁴Dipartimento di Fisica, Università di Roma Tor Vergata, Via della Ricerca Scientifica, 00133 Roma, Italy

E-mail: silvia.gagliardini@roma1.infn.it

Abstract. The recently discovered TeV emission from Gamma-Ray Bursts (GRBs) hints towards a possible hadronic origin of this radiation component. We developed a Monte Carlo (MC) simulation reproducing the kinematics of photo-hadronic interactions at internal shocks, including the pair production process that the secondary gamma rays undergo in the GRB jet. We find that sub-TeV observations of GRB 190114C can be reproduced by a baryonic energy content comparable to that in sub-GeV photons and a bulk Lorentz factor $\Gamma = 100$, with a ms variability timescale. Neutrino flux predictions by the model are found to be consistent with experimental upper limits set by ANTARES and IceCube.

Keywords: Gamma-ray bursts; neutrinos; radiation; simulations

Contents

1	Introduction	1
2	GRB 190114C: spectral and temporal properties	1
3	Monte Carlo simulation	2
4	Results: gamma rays and neutrinos from photo-hadronic interactions	5
5	Discussion and Conclusions	7

1 Introduction

GRB 190114C is the first long-duration GRB observed to emit gamma rays in the TeV band. Indeed, MAGIC detected from this GRB high-energy gamma rays (0.2–1 TeV) with high significance, at the transition between the prompt and afterglow phases of the GRB emission [1]. A purely leptonic scenario consisting of synchrotron self-Compton radiation produced at external shocks does not match the broadband emission observed in GRB 190114C [2]. In addition, the large number of parameters involved in the model highly limits its prediction power. Although firm conclusions on the production mechanisms of GeV–TeV emission have been reached so far [3–9], the hypothesis that part of this emission could be caused by the presence of a hadronic component cannot be excluded [4, 6, 7], with the subsequent production of high-energy neutrinos [10–13].

We test a scenario in which the very high-energy (VHE) emission of GRB 190114C is due to photo-hadronic interactions occurring in the GRB jet during the prompt phase. We consider the standard fireball model in which energy dissipation occurs at shocks internally to the relativistic outflow of the jet or through interactions with ambient matter [10, 11]. Thus, a substantial part of the bulk kinetic energy is converted into internal energy, which is then distributed between electrons, protons, and magnetic field. The internally accelerated electrons are presumably responsible for the keV–GeV photons observed in the GRB, which are emitted through synchrotron or inverse Compton processes. Accelerated protons may interact with these photons (\sim MeV) and produce both neutral and charged pions, which in turn decay, originating, respectively, high-energy photons and neutrinos.

The paper is structured as follows: in Sec. 2 we introduce the spectral and temporal properties of GRB 190114C. In Sec. 3 we present our MC simulation, developed to describe the physics of photo-hadronic interactions occurring in the internal shock (IS) region of the GRB jet. In Sec. 4 we compare the photon flux resulting from our simulation to the Extragalactic Background Light (EBL) deconvolved MAGIC data, obtaining a set of best fit values of the model parameters. We then predict a flux of high energy neutrinos and evaluate the expected number of events in present and future experiments. A discussion of our results is provided in Sec. 5.

2 GRB 190114C: spectral and temporal properties

GRB 190114C was the first GRB detected at sub-TeV energies, among the few observed so far. The combination of a rapid follow-up by MAGIC [14] with the close distance of the

source (confirmed from its optical counterpart to be at redshift $z = 0.4245$ [15, 16]) allowed to unveil the presence of an extremely energetic radiation component in GRBs, long before theorised [17]. In the gamma-ray band, after the trigger by Swift [18], further observations have followed by GBM [19] and LAT [20] onboard the *Fermi* satellite (up to 22.9 GeV), AGILE/MCAL [21], Integral/SPI-ACS [22] and Konus-Wind [23].

The prompt phase of GRB 190114C, as observed by Fermi-GBM, appears as a multi-peak emission lasting $T_{90} \simeq 116$ s (50-300 keV). The time-averaged spectrum in the first ~ 40 s can be described by a Band function with low and high-energy slopes equal to $\alpha = 1.058$ and $\beta = 3.18$, respectively, a break energy value of $E_b \simeq 1.1$ MeV in the observed frame [19], and a gamma-ray fluence of $F_\gamma = 3.99 \times 10^{-4}$ erg cm $^{-2}$ (10-1000 keV). As such, the isotropic energy release in the source frame amounts to $E_{\text{iso}} \simeq 3 \times 10^{53}$ erg, indicating a fairly energetic (though not the most extreme) GRB. In turn, MAGIC detection occurred 68 s after the Fermi-GBM trigger, with a significance above 50σ : VHE emission lasted for ~ 40 minutes, with the highest observed photon energy of $E_{\text{max}} = 0.852$ TeV [1]. Within this temporal window, the time-dependent analysis of VHE data showed a systematic decrease in flux normalization, as well as a steepening trend over time. The high-energy photon spectrum reported by MAGIC for the time interval 68-110 s entirely overlaps with the T_{90} estimated by Fermi-GBM for the prompt emission. During this time interval, the intrinsic burst spectrum in the 0.2-1 TeV band is characterised by a pure power-law ($\propto E^{-\xi}$) with $\xi = 2.16_{-0.31}^{+0.29}$ [2]. The photon spectral slope at the source has been derived taking into account the severe attenuation of the gamma ray flux due to its propagation to the Earth within the EBL [2], according to the Dominguez et al. model [24]. We hence consider such an intrinsic spectrum and we compare it with the prediction of the gamma-ray flux emerging from our simulation of the IS region. Additionally, we investigated the effects of adopting a different EBL model, e.g. that from Franceschini et al. [25, 26], finding results consistent with the Dominguez et al. model within the statistical uncertainty of the MAGIC measurements.

The temporal overlap between the MAGIC observations and T_{90} is not sufficient to definitely attribute the high-energy photons measured by MAGIC to the prompt or to the afterglow phase of the GRB emission. We here consider the radiation emerging from hadronic interactions occurring at the IS region between accelerated protons and the Band-like target radiation field. The two main features of a hadronic scenario are Γ , and the amount of energy channeled into relativistic protons $E_{\text{iso,p}}$, which can be expressed with the baryon loading $f_p = E_{\text{iso,p}}/E_{\text{iso}}$. Both the values of Γ and f_p can be constrained to reproduce the VHE spectrum in terms of hadronic gamma rays.

Concerning the value of Γ , we estimate the minimum Γ required by a $E_\gamma \simeq 1$ MeV photon to be revealed at Earth, as observed by Fermi-GBM. This can be constrained by requiring that the optical thickness τ for pair production $\gamma\gamma \rightarrow e^+e^-$ be $\tau \leq 1$. Following [27], we calculated the total number of photons emitted during the first ~ 40 s, with energy greater than $E_{\text{max,pair}} = (2\Gamma m_e c^2)^2/E_\gamma$, for different variability times $t_{\text{var}} = 6, 3, 1$ ms [28–30], obtaining minimum Lorentz factor values $\Gamma_{\text{min}} \simeq 60, 70, 90$, respectively.

3 Monte Carlo simulation

Modeling the physical processes occurring inside the IS region of the expanding GRB fireball requires characterization of the site where particles propagation and interactions take place. Here we consider a simplified stationary one-zone scenario [31–33], in which mildly relativistic

shells of plasma collide at a typical radius [34]

$$R_{\text{IS}} = \frac{2\Gamma^2 ct_{\text{var}}}{(1+z)} \simeq 4 \times 10^{12} \left(\frac{\Gamma}{100} \right)^2 \left(\frac{t_{\text{var}}}{0.01 \text{ s}} \right) \left(\frac{1.4}{1+z} \right) \text{ cm}. \quad (3.1)$$

In our simulation, we assume variability timescale values t_{var} ranging from 1 to 6 ms, the latter being suggested by observations during the prompt phase of GRB 190114C [28]. In turn, Γ is treated as a free parameter of the model, whose most likely value will be fixed as the one that best reproduces MAGIC data.

The MC calculation is performed in the IS frame, assuming a spherical geometry [35]. The total fluence is considered to result from N interaction regions, where $N = T_{90}/t_{\text{var}}$. The shell width, in the IS frame, is given by $\Delta R_{\text{IS}} = N\Gamma ct_{\text{var}}/(1+z)$. The process relies on the generation of accelerated protons, with energy range $1 - 10^9$ GeV, characterized by a differential energy spectrum according to $dN_{\text{p}}/dE_{\text{p}} \propto E_{\text{p}}^{-2}$, consistently with a Fermi I-order acceleration process. Although we consider internal shocks within the fireball model as location for particle acceleration, several other processes have been suggested in literature to possibly energize particles in extremely relativistic jets, as magnetic reconnection [36–38]. The target photon energy distribution in the IS frame is assumed to reproduce the Band function observed by Fermi-GBM [19] in the prompt phase, and has been extended to higher energies, in order to allow the particle Δ^+ resonance¹ production with the entire spectrum of accelerated protons.

Each generated proton can either interact with ambient photons if the center of mass energy is above the interaction threshold condition or it propagates further in the shell. The interaction length $\lambda_{p\gamma}(s) = [n_{\gamma}\sigma_{p\gamma}(s)]^{-1}$ is evaluated, depending on the $p\gamma$ center of mass energy, and on the density of photons in the IS frame $n_{\gamma}(\epsilon_{\text{th},\Delta}^{\text{IS}})$ allowing a center of mass energy above the Δ^+ production, namely such that $\epsilon_{\text{th},\Delta}^{\text{IS}} = (m_{\Delta}^2 - m_{\text{p}}^2)c^4/(4E_{\text{p}}^{\text{IS}})$, (m_{Δ} and m_{p} being respectively the Δ^+ and proton masses).

A mean free path x_{p} is assigned to each proton, as in [39]: if $x_{\text{p}} < R_{\text{IS}}$ and if the threshold condition for the Δ^+ production is satisfied, the photo-meson interaction occurs. The energies of protons (E_{p}^{IS}) and photons ($\epsilon_{\gamma}^{\text{IS}}$) that satisfy the photo-meson production condition are shown in Fig. 1.

Multi-pion generation beyond resonant Δ^+ production is also simulated. Particles like $\pi^0, \pi^{\pm}, \mu^{\pm}, \nu_{\mu}, \bar{\nu}_{\mu}, \nu_e, \bar{\nu}_e$, as well as secondary protons originated by the interaction, are followed by the simulation. The secondary protons are tracked until they leave the IS region to account for possible re-interactions along their path with the same target photon spectrum. Pions and muons are followed until they decay.

To account for energy losses of charged particles within the propagation timescale inside the IS region, we introduce purely exponential spectral cut-offs on top of their power-law distributions: the steady state energy distribution for protons is obtained by comparing the acceleration timescale $t_{\text{acc}}(E_{\text{p}}^{\text{IS}}) = r_{\text{L}}(E_{\text{p}}^{\text{IS}})/c$, being r_{L} the particle Larmor radius, to the average inelastic collision timescale for the Δ -baryon production $t_{p\gamma}(E_{\text{p}}^{\text{IS}}) = [n_{\gamma}(\epsilon_{\text{th},\Delta}^{\text{IS}})c\sigma_{p\gamma}^{\Delta}K_{p\gamma}]^{-1}$. In the previous expression, $K_{p\gamma} = 0.13$ and $\sigma_{p\gamma}^{\Delta} = 5 \times 10^{-28} \text{ cm}^2$ are respectively the inelasticity and the cross section of the interaction at the threshold [40]. Adiabatic and synchrotron losses have negligible impact on protons, i.e. for $\Gamma = 100$ and $t_{\text{var}} = 1$ ms we find that the proton cut-off energy amounts to $E_{\text{p,cut}}^{\text{IS}} \simeq 2.4$ PeV.

As muons and charged pions could be affected by synchrotron losses, we evaluated the

¹Mass $m_{\Delta} = 1232 \text{ MeV}/c^2$, spin $S = 0$, isospin $I = 3/2$, total angular momentum $J = 3/2$, parity $P = +$.

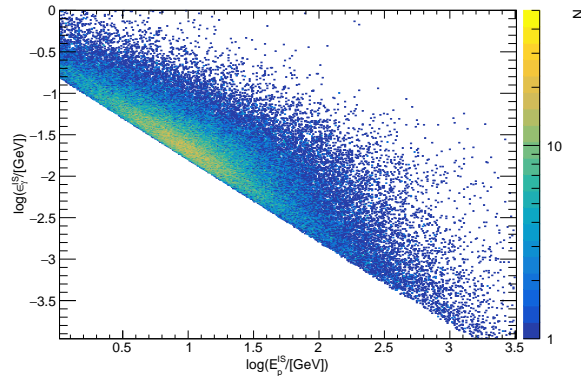


Figure 1. Distribution of simulated events exceeding the photo-meson threshold in the IS frame ($\Gamma = 100$ and $t_{\text{var}} = 1$ ms): the x-axis refers to accelerated proton energies, while the y-axis refers to target photon energies.

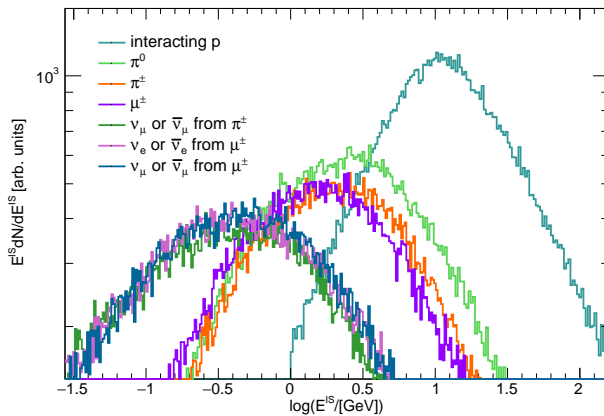


Figure 2. Particle spectra resulting from $p\gamma$ interactions, obtained in the IS frame from the simulation with $\Gamma = 100$ and $t_{\text{var}} = 1$ ms.

magnetic field value at IS by equating the magnetic energy density $U_B = B^2/(8\pi)$ with the kinetic energy density of the accelerated electrons. Naming ϵ_B and ϵ_e the fraction of jet energy converted into magnetic energy and carried by electrons, respectively, we assume $\epsilon_e = \epsilon_B = 0.1$. Pion and muon lifetimes are longer than the synchrotron timescale $t_{\text{syn}}(E^{\text{IS}}) = 9m^4/(4cq_e^4 E^{\text{IS}} B^2)$ for IS energies, respectively, above $E_{\mu^\pm, \text{cut}}^{\text{IS}} \simeq 0.5$ TeV and $E_{\pi^\pm, \text{cut}}^{\text{IS}} \simeq 9$ TeV ($\Gamma = 100$, $t_{\text{var}} = 1$ ms).

The kinematics of $p\gamma$ interactions follows the methods in [39]. The energy particle distribution for interacting protons, charged pions, muons and neutrinos assuming $\Gamma = 100$ and $t_{\text{var}} = 1$ ms is shown in Fig. 2.

Concerning the neutral pion production and decay, we consider the possibility that each originated gamma ray might further interact within the IS shell with low-energy ambient photons, via e^\pm pair production. The radiation length of this process is evaluated as $\lambda_{\gamma\gamma}(s') = [n_\gamma(\epsilon_{\text{th}, e^\pm}^{\text{IS}})\sigma_{\gamma\gamma}(s')]^{-1}$, where s' is the $\gamma\gamma$ center of mass energy squared, $\sigma_{\gamma\gamma}$ is the e^\pm pair production cross section [41], and $\epsilon_{\text{th}, e^\pm}^{\text{IS}}$ is the target photon threshold energy. The target

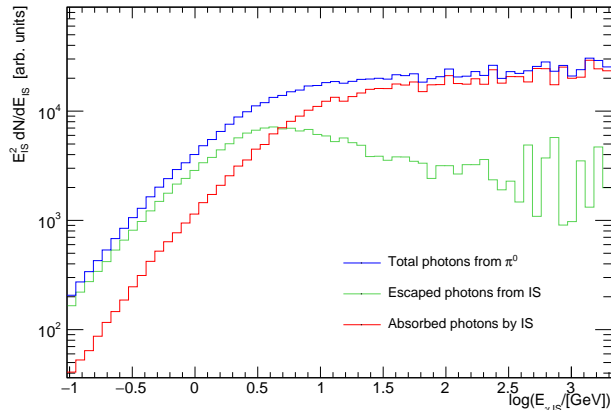


Figure 3. Spectral Energy Density (SED) obtained from the simulation with $\Gamma = 100$ and $t_{\text{var}} = 1$ ms in the Internal Shock frame: in blue the total photons from π^0 decay, in red and in green respectively the absorbed and the escaped ones.

photon is extracted from a uniformly distributed angle $\cos\theta$ with respect to the gamma ray. For each gamma with energy E_γ^{IS} originated from π^0 decay, we extract its mean free path x_γ according to the radiation length $\lambda_{\gamma\gamma}$, and if $x_\gamma < R_{\text{IS}}$, we evaluate whether or not the e^\pm pair production threshold condition is satisfied [41]:

$$E_\gamma^{\text{IS}} \geq \frac{2m_e^2 c^4}{\epsilon^{\text{IS}}(1 - \cos\theta)} \simeq \frac{1.02}{\epsilon_{eV}^{\text{IS}}(1 - \cos\theta)} \text{ TeV}. \quad (3.2)$$

For our purposes, the Band spectrum of target photons is assumed to extend outside of the Fermi-GBM observed energy range, to allow the pair production to occur with the gamma ray originated from π^0 -decay.

We find that only $\simeq 40\%$ of the 10 GeV gamma rays in the IS frame ($\Gamma = 100$ and $t_{\text{var}} = 1$ ms) will survive the e^\pm production process, see Fig. 3. At fixed gamma-ray energy, the effect of $\gamma\gamma$ absorption is larger for lower values of Γ , since the target photon density increases lowering Γ . The emerging photons will eventually be observed in the laboratory frame with energy $E_{\text{obs}} = \Gamma E_{\text{IS}}/(1+z)$. The flux of escaping photons can be directly compared with the intrinsic Spectral Energy Density (SED) derived by MAGIC.

4 Results: gamma rays and neutrinos from photo-hadronic interactions

We perform MC simulation for different values of t_{var} and Γ , obtaining spectra of high-energy gamma rays and neutrinos emerging from the interaction region. We then converted these spectra into expected fluxes on Earth by taking into account the cosmological nature of GRBs. For the particle energy flux $E^2\phi(E)$, either photons or neutrinos, we rescaled the IS energy spectrum through: i) the comoving distance $d_c = d_L/(1+z)$, where d_L represents the luminosity distance, ii) the first time interval of MAGIC observations $\Delta t = 42$ s, and iii) the energy conversion factor from the IS to the observed frame, as:

$$E^2\phi(E) = f_p \Gamma \frac{(1+z)}{4\pi d_L^2 \Delta t} \left(E^2 \frac{dN}{dE} \right)_{\text{IS}}. \quad (4.1)$$

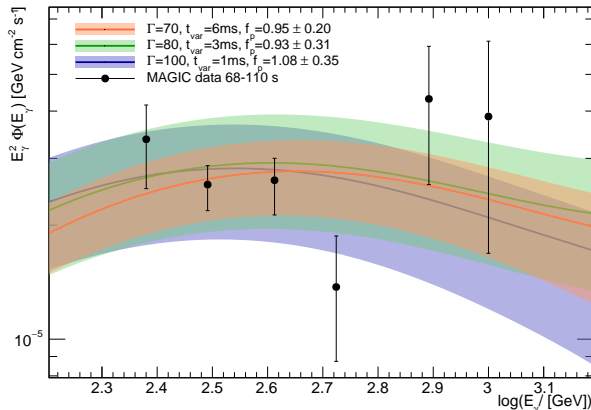


Figure 4. Comparison between the EBL-deconvolved flux of GRB 190114C, as provided by MAGIC in the temporal interval 68-110 s [2], and the simulated photon flux arising from the π^0 -decay, after accounting for internal gamma-ray absorption, for different parameters of the model.

For each simulated Γ and t_{var} , the baryon loading f_p has been varied in the interval 0.1–5.0 in uniform steps of width $\Delta f_p = 0.1$, to derive the best agreement between the EBL-deconvolved MAGIC data in the 68-110 s time interval [2] and the simulated fluxes, through a χ^2 statistical test. Considering the Γ values dictated by the opacity argument (see Sec. 2), for $t_{\text{var}} = 1, 3, 6$ ms we obtain $\Gamma = 100, 80, 70$ and $f_p = 1.10, 0.93, 0.95$ as best-fit parameters. Remarkably, despite the broad variation in the values of Γ characterizing the models that possibly reproduce sub-TeV data, an almost constant f_p is obtained, suggesting a comparable amount of energy being channeled in the hadronic and leptonic jet components. By fixing Γ to the best-fit value, we evaluated the statistical uncertainty on flux normalisation. This result is shown in Fig. 4, where the modellings that best reproduce the EBL-deconvolved MAGIC data are reported, the shaded area representing the 1σ statistical uncertainty evaluated over f_p .

A direct proof of the hadronic origin of the observed TeV radiation might come from coincident neutrino observations. Because of the transient nature of GRBs, the detection of a single neutrino event would allow identifying these sources as extreme hadronic accelerators. Despite the experimental efforts, no clear signal has emerged so far in data from the ANTARES and IceCube telescopes [42] [43], when searching for spatial and temporal coincidences with the prompt emission of GRBs. This leads to a constraint on the possible contribution of standard GRBs to less than 10% of the diffuse cosmic neutrino flux [44–47]. Furthermore, it is still unclear whether TeV-emitting GRBs behave as the standard GRB population. Both the ANTARES and IceCube Collaborations have unsuccessfully searched for coincident neutrino-induced signals from the direction of GRB 190114C. In the case of ANTARES, the derived 90% confidence level integrated upper limit amounts to 1.6 GeV/cm^2 , while for IceCube it is 0.44 GeV/cm^2 [48, 49]. In both cases, the constraints are limited to the muon neutrino component reaching Earth. In fact, because angular precision is a crucial feature in reducing the atmospheric background entering the search cone angle, muon neutrino charged-current interactions constitute the better astronomical channel, as muons emerging from these can be identified in neutrino telescopes as long tracks.

To evaluate the neutrino energy flux on Earth for muon neutrinos and antineutrinos

we took into account neutrino oscillations (normal ordering case in the standard three-flavor scenario [50]). Current neutrino detectors ANTARES and IceCube have analysed their data sample looking for possible spatially coincident neutrino signals; however, the resulting upper limits are a few orders of magnitude above the model predictions here presented, indicating that the non-detection of current instruments is compatible with the hadronic model expectations for the values of f_p and Γ that better reproduce the sub-TeV gamma-ray MAGIC data. To understand whether present and future neutrino detectors might be able to find a signal comparable to the one expected from a GRB similar to GRB 190114C, having obtained the muon neutrino (and antineutrino) fluence $dN_{\nu_\mu}/(dE_{\nu_\mu}dS)$, we can compute the expected number of track-like events:

$$N_{\text{events}}(\delta) = \int A_{\text{eff}}^{\nu_\mu}(E_\nu, \delta) \left(\frac{dN_{\nu_\mu}}{dE_{\nu_\mu}dS} \right)_{\text{Earth}} dE_{\nu_\mu}, \quad (4.2)$$

where the neutrino telescope effective area $A_{\text{eff}}^{\nu_\mu}$ is a function of the neutrino energy and of the source declination δ . Public effective areas of ANTARES [42] and IceCube [43] are evaluated at analysis level and for the declination band that includes the position of GRB 190114C. For KM3NeT/ARCA the effective area is evaluated at trigger level and averaged throughout the sky [51]. In Fig. 5 we report the number of muon neutrino and antineutrino expected events for the 3 neutrino detectors as a function of the neutrino energy.

In Table 1, we report the expected total number of neutrino-induced events in the three large-volume detectors relative to the simulation with $t_{\text{var}} = 1$ ms, $\Gamma = 100$ and $f_p = 1.1$. Although the coincident background rate due to atmospheric neutrinos is by orders of magnitude lower than the signal rate expected from GRB 190114C, a detection from a single GRB appears to be very difficult. This result suggests that stacking several GRBs of the same kind could be the only viable solution for a significant detection.

Detector	Declination band	N_{events}
ANTARES	$-45^\circ < \delta < 0^\circ$	1×10^{-3}
IceCube	$-30^\circ < \delta < 0^\circ$	2×10^{-2}
KM3NeT/ARCA	Average	1×10^{-1}

Table 1. Signal events expected in different neutrino telescopes, as induced by ν_μ and $\bar{\nu}_\mu$ interactions during the [68;100] s time interval of the prompt emission of GRB 190114C, for the model with $t_{\text{var}} = 1$ ms, $\Gamma = 100$ and $f_p = 1.1$.

5 Discussion and Conclusions

The successful observation of radiation from GRBs extending up to the TeV domain has provided further evidence of the extreme nature of these sources. However, there is still poor understanding of the processes that characterize the observed TeV emission emerging from GRB 190114C (and the few others detected at TeV energies). The newly discovered radiation component might witness the presence of effective hadronic acceleration in GRB jets, possibly already during the prompt phase of the emission. This occurrence would establish the connection between GRBs and Ultra-High-Energy Cosmic Rays (UHECRs), which remains a long-standing paradigm still to be proven.

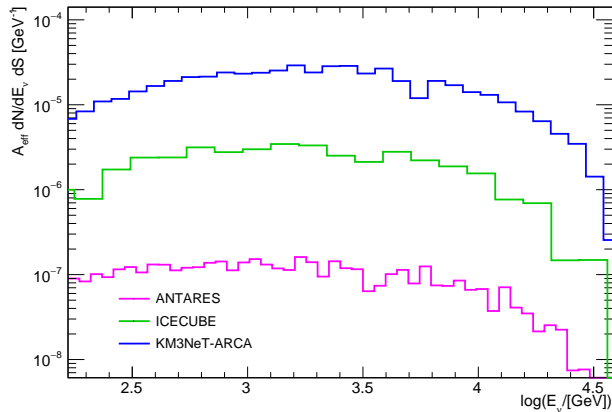


Figure 5. Number of expected muon neutrino and antineutrino events, for each energy bin, from GRB190114C for $\Gamma=100$ and $t_{var} = 1$ ms: magenta for ANTARES [42], green for Icecube [43], blue for KM3NeT/ARCA [51].

To test the hypothesis of the hadronic origin of TeV radiation, we developed a MC simulation of photo-meson interactions between high-energy protons and target photons distributed according to a Band-like spectrum, as indicated by Fermi-GBM observations. After computing the spectra of secondary particles emerging from these interactions, we additionally simulated the electromagnetic absorption that gamma rays undergo in the IS shell. The spectrum of escaping photons thus obtained has been compared to the intrinsic source spectrum derived by deconvolving MAGIC observations of GRB 190114C in the EBL. The free parameters of the hadronic model have been constrained by means of a residual minimization procedure, indicating that the source channeled a comparable amount of energy into photons and hadrons. Extended studies about the entire sample of observed TeV GRBs are required to understand the physical mechanisms responsible for the TeV emission. In particular, it appears to crucial to have a better characterization of the very-high-energy photon spectrum in the early stages of the GRB emission, which seems to be currently limited by the prompt response of imaging atmospheric Cherenkov telescopes in pointing. Confirmation of the hadronic origin of sub-TeV radiation might, in principle, arise from neutrino observations. In the context of the parameters that better reproduce MAGIC data, however, such a detection from GRB 190114C appears extremely unrealistic, as confirmed by the lack of spatial correlations in data from both the ANTARES and IceCube neutrino telescopes.

Acknowledgments

The authors acknowledge the support of the Amaldi Research Center funded by the MIUR programme “Dipartimento di Eccellenza” (CUP:B81I18001170001), the Sapienza School for Advanced Studies (SSAS) and the support of the Sapienza Grants No. RM120172AEF49A82 and RG12117A87956C66. The authors are thankful to Enrico Peretti for fruitful discussions regarding the manuscript content.

References

- [1] V. A. Acciari et al. (MAGIC Collaboration), Nature 575 (2019) 455

- [2] V. A. Acciari et al. (MAGIC Collaboration), *Nature* 575 (2019) 459
- [3] M. E. Ravasio, G. Oganesyan, O. S. Salafia, G. Ghirlanda, G. Ghisellini, M. Branchesi, S. Campana, S. Covino & R. Salvaterra, *A&A* 626 (2019) 12
- [4] N. Fraija, R. Barniol Duran, S. Dichiara & P. Beniamini, *ApJ* 883 (2019b) 162
- [5] X. Y. Wang, R. Y. Liu, H. M. Zhang, S. Q. Xi and B. Zhang, *ApJ* 884 (2019) 117
- [6] E. Derishev & T. Piran, *ApJ*, 880, (2019), 27
- [7] S. Sahu, & C. E. López Fortín, *ApJL* 895 (2020) L41
- [8] V. Chand, P. S. Pal, A. Banerjee, V. Sharma, P. H. T. Tam, and X. He, *ApJ* 903 (2020) 9
- [9] J. A. Rueda, R. Ruffini, M. Karlica, R. Moradi & Y. Wang, *ApJ* 893 (2020) 148
- [10] D. Eichler, D. Guetta & M. Pohl, *ApJ* 722 (2010) 543
- [11] D. Guetta, M. Spada & E. Waxman, *ApJ* 559 (2001) 101
- [12] D. Guetta, *JHEAp*, 7, 90 (2015)
- [13] L. Yacobi, D. Guetta & E. Behar, *ApJ* 793 (2014) 48
- [14] R. Mirzoyan et al., *ATel* 12390 (2019) 1
- [15] J. Selsing et al. (NOT Collaboration) *GCN* 23695 (2019)
- [16] A. J. Castro-Tirado et al. (GTC Collaboration) *GCN* 23708 (2019)
- [17] E. V. Derishev, V. V. Kocharovsky & V. V. Kocharovskya, *Advances in Space Research (ASR)* 27 (2001) 813-818
- [18] J. D. Gropp et al. (Swift Collaboration) *GCN* 23688 (2019)
- [19] R. Hamburg et al. (Fermi-GBM Collaboration), 2019, *GCN* 23707
- [20] D. Kocevski et al. (Fermi-LAT Collaboration), 2019, *GCN* 23709
- [21] A. Ursi et al. (AGILE Collaboration), *GCN* 23712 (2019)
- [22] P. Minaev & A. Pozanenko, *GCN* 23714 (2019)
- [23] D. Frederiks et al. (Konus-Wind Collaboration), *GCN* 23737 (2019)
- [24] A. Dominguez et al., *Mon. Not. R. Astron. Soc.* 41 (2011) 2556–2578
- [25] A. Franceschini & G. Rodighiero, *A&A* 603 (2017) A34
- [26] A. Franceschini & G. Rodighiero, *A&A* 614 (2018) C1
- [27] Y. Lithwick & R. Sari, *The Astrophysical Journal* 555 (2001) 1
- [28] M. Ajello et al., *ApJ*, 890, (2020), 9
- [29] V. Zach Golkhou et al., *ApJ*, 811, (2015), 93
- [30] G. A. MacLachlan et al., *MNRAS* 432, 857–865 (2013)
- [31] K. Murase & S. Nagataki, *Phys. Rev. D* 73 (2006) 063002
- [32] K. Asano, S. Inoue & P. Meszaros, *ApJ*, 699, (2009), 953
- [33] S. Hummer, P. Baerwald & W. Winter, *Phys. Rev. Lett.* 108 (2012) 231101
- [34] P. Baerwald, M. Bustamante, K. Murase & W. Winter, *Nat. Commun.* 6 (2015) 6783
- [35] P. Baerwald, S. Hummer & W. Winter, *Astropart. Phys.* 35 (2012) 508
- [36] B. Zhang & H. Yan, *ApJ* 726 (2011) 2
- [37] D. Giannios, D. A. Uzdensky and Mitchell C. Begelman, *MNRAS* 395 (2009) 1

- [38] T. E. Medina-Torrejón, E. M. de Gouveia Dal Pino, L. H. S. Kadowaki, G. Kowal, C. B. Singh & Y. Mizuno, *ApJ* 908 (2021) 193
- [39] M. Fasano, S. Celli, D. Guetta, A. Capone, A. Zegarelli & I. Di Palma, *JCAP* 09 (2021) 044
- [40] A. Atoyan & C.D. Dermer, *Phys. Rev. Lett.* 87 (2001) 221102
- [41] S. Vernetto and P. Lipari, *Phys. Rev. D* 94 (2016) 063009
- [42] S. Adrian-Martínez et al. (ANTARES Collaboration), *Astrophys. J.* 760 (2012) 53
- [43] M. G. Aartsen et al. (IceCube Collaboration), *ApJ.* 796 (2014) 109
- [44] S. Adrian-Martínez et al. (ANTARES Collaboration), *Astron. Astrophys.* 559 (2013) A9
- [45] A. Albert et al. (ANTARES Collaboration), *Mon. Not. R. Astron. Soc.* 469 (2017) 906
- [46] A. Albert et al. (ANTARES Collaboration), *Mon. Not. R. Astron. Soc.* 500 (2021) 5614
- [47] M. G. Aartsen et al. (IceCube Collaboration), *ApJ.* 843 (2017) 112
- [48] A. Albert et al. (ANTARES Collaboration), *JCAP* 03 (2021) 092
- [49] J. Vandenbroucke et al. (IceCube Collaboration), *ATel* 12395 (2019)
- [50] C. Mascaretti & F. Vissani, *JCAP* 08 (2019) 004
- [51] S. Adrian-Martinez et al. (KM3NeT Collaboration), *J. Phys. G: Nucl. Part. Phys.* 43 (2016) 084001